THE JOURNAL OF BIOLOGICAL CHEMISTRY VOL. 287, NO. 49, pp. 41218–41231, November 30, 2012

Headpiece Domain of Dematin Regulates Calcium Mobilization and Signaling in Platelets*[S]

Received for publication, March 21, 2012, and in revised form, October 10, 2012 Published, JBC Papers in Press, October 11, 2012, DOI 10.1074/jbc.M112.364679

Adam J. Wieschhaus[‡§¶], **Guy C. Le Breton**[¶], **and Athar H. Chishti**[‡1]

From the [‡]*Department of Molecular Physiology and Pharmacology and the* [§]*Programs in Physiology, Pharmacology, and Microbiology, Sackler School of Graduate Biomedical Sciences, Tufts University School of Medicine, Boston, Massachusetts 02111 and the* [¶]*Department of Pharmacology, University of Illinois College of Medicine, Chicago, Illinois 60612*

Background: Dematin is a major component of the erythrocyte membrane. Its abundance in platelets suggests a conserved function.
Results: Dematin regulates calcium mobilization in platelets. Mice lacking the dematin headpiece domain show multiple defects in platelet function.
Conclusion: Dematin emerges as a new regulator of calcium mobilization in platelets.
Significance: Inhibition of dematin interactions may offer new therapeutic approaches against platelet activation and cardiovascular diseases.

Dematin is a broadly expressed membrane cytoskeletal protein that has been well characterized in erythrocytes and to a lesser extent in non-erythroid cells. However, dematin's function in platelets is not known. Here, we show that dematin is abundantly expressed in both human and mouse platelets. Platelets harvested from the dematin headpiece knock-out (HPKO) mouse model exhibit a striking defect in the mobilization of calcium in response to multiple agonists of platelet activation. The reduced calcium mobilization in HPKO platelets is associated with concomitant inhibition of platelet aggregation and granule secretion. Integrin $\alpha_{IIb}\beta_3$ activation in response to agonists is attenuated in the HPKO platelets. The mutant platelets show nearly normal spreading on fibrinogen and an unaltered basal cAMP level; however, the clot retraction was compromised in the mutant mice. Immunofluorescence analysis indicated that dematin is present both at the dense tubular system and plasma membrane fractions of platelets. Proteomic analysis of dematin-associated proteins in human platelets identified inositol 1,4,5-trisphosphate 3-kinase isoform B (IP3KB) as a binding partner, which was confirmed by immunoprecipitation analysis. IP3KB, a dense tubular system protein, is a major regulator of calcium homeostasis. Loss of the dematin headpiece resulted in a decrease of IP3KB at the membrane and increased levels of IP3KB in the cytosol. Collectively, these findings unveil dematin as a novel regulator of internal calcium mobilization in platelets affecting multiple signaling and cytoskeletal functions. Implications of a conserved role of dematin in the regulation of calcium homeostasis in other cell types will be discussed.

Dematin, also known as protein 4.9, is a peripheral membrane protein that links the spectrin-actin junctions to the plasma membrane in erythrocytes (1, 2). Dematin is also a substrate of multiple protein kinases, and phosphorylation by cAMP-dependent protein kinase reversibly abolishes its actin bundling function *in vitro* (3, 4). The primary structure of dematin includes a carboxyl-terminal domain with sequence similarity to the headpiece domain found in the villin-type family of cytoskeletal proteins (2). The amino-terminal core domain of dematin shows sequence similarity to the LIM domain-containing proteins termed ABLIMs (5). Biophysical measurements, including nuclear magnetic resonance studies of dematin, have shown a fully folded headpiece domain linked to a primarily unfolded core domain (6, 7). Native dematin purified from human erythrocyte membranes forms a trimer in solution composed of two polypeptides of 48 kDa and one polypeptide of 52 kDa (4, 8). These two isoforms of dematin are generated by alternative splicing of a single gene located on human chromosome 8p21 (9). The 48-kDa isoform of dematin, composed of 383 amino acids, predicts a protein with an isoelectric point of 9.54, whereas the 52-kDa isoform consisting of 405 amino acids is generated by the 22-amino acid insertion within the headpiece domain (2). It is to be noted that although the 383 amino acids of dematin predict a protein of 43 kDa, the two isoforms of dematin isolated from erythrocytes migrate as 48 and 52 kDa bands on SDS-polyacrylamide gels (3). This anomalous electrophoretic migration is probably due to the presence of a cluster of negatively charged residues within the core domain shared between the two isoforms of dematin (2). The headpiece domain contains the major actin-binding site, whereas the core domain contains a second actin-binding site as well as mediates dematin's interactions with the plasma membrane (1, 9, 10).

Dematin is located at the spectrin-actin junctions in the erythrocyte membrane (11). The spectrin-actin junctions, also called the junctional complex, are critical for maintaining the mechanical properties of the erythrocyte membrane. These junctions are assembled by a multiprotein complex consisting

* This work was supported, in whole or in part, by National Institutes of Health Grants HL095050, HL089517, and HL051445 (to A. H. C.) and HL24530 (to G. C. L.).
[S] This article contains supplemental Figs. S1 and S2.
[1] To whom correspondence should be addressed: Dept. of Molecular Physiology and Pharmacology, Tufts University School of Medicine, 150 Harrison Ave., Rm. 701A, Boston, MA 02111. Tel.: 617-636-3457; Fax: 617-636-3568; E-mail: athar.chishti@tufts.edu.

of spectrin, actin, dematin, adducin, protein 4.1R, tropomyosin, tropomodulin, calmodulin, and p55/MPP1. This multiprotein complex is linked to the plasma membrane by several transmembrane proteins, including glycophorin C, band 3, and GLUT1 (glucose transporter-1), in a species-specific manner (1, 12). To determine the physiological function of dematin *in vivo*, we generated a dematin headpiece knock-out (HPKO)[2] mouse model (2). The HPKO mice are characterized with defects in erythrocyte shape, membrane stability, and membrane cytoskeletal interactions (2). Later, we generated a double knock-out (DKO) mouse model lacking both the headpiece domain of dematin and β-adducin (10). The DKO mice exhibit severe hemolytic anemia with striking abnormalities in erythrocyte shape and membrane stability (10). These findings demonstrated that dematin and adducin perform a critical overlapping function at the spectrin-actin junctions, regulating erythrocyte shape and membrane stability *in vivo* (10).

Despite our improved understanding of dematin function in mature erythrocytes, its function in non-erythroid cells has just begun to be appreciated. Dematin is a widely expressed protein with immunoreactive polypeptides present in heart, brain, skeletal muscle, lung, and kidney (2, 13). Using the HPKO mouse model, we recently demonstrated that dematin headpiece domain deletion results in impaired wound healing *in vivo*, delayed cell migration, and enhanced fibroblast adhesion (14, 15). Moreover, dematin was identified as a suppressor of RhoA activation in the mouse fibroblasts (14, 15), consistent with the role of the ABLIM family of proteins in the regulation of Rho family of GTPases and the actin cytoskeleton (16). Interestingly, both adducin and RhoA have been functionally implicated in the regulation of the actin cytoskeleton and signaling pathways in platelets (17, 18). In this paper, we provide evidence that dematin is abundantly expressed in platelets and functions as a novel regulator of calcium homeostasis. The HPKO mice display multiple defects in platelet functions, thus unveiling dematin as an important regulator of the cytoskeleton and signaling pathways in platelets.

EXPERIMENTAL PROCEDURES

Isolation of Platelets—Blood was collected from healthy human donors and adult mice. Generally, 5–6 wild type (WT) and HPKO mice were anesthetized by inhalation of 3% isoflurane, and blood was collected from the inferior vena cava. Blood was anticoagulated with ⅐ volume (~15%) of ACD (85 mM trisodium citrate, 83 mM dextrose, and 21 mM citric acid) and platelet-rich plasma (PRP) was harvested by centrifugation of the blood at 180 × *g* for 15 min at room temperature. The PRP was centrifuged for 10 min at 600 × *g* in the presence of 0.1 μg/ml prostaglandin E_1 and 5 mM EDTA. Washed platelets were resuspended in modified Tyrode's buffer (10 mM HEPES, 12 mM $NaHCO_3$, 137 mM NaCl, 2.5 mM KCl, 5.0 mM glucose, 1.0 mM $MgCl_2$, and 0.35% BSA). Platelets were allowed to rest for 60 min, and 1.0 mM $CaCl_2$ was added prior to the start of each experiment.

Western Blotting—Western blotting of dematin in human (3×10^8 platelets/ml) and mouse (2×10^8/ml) platelets was performed using multiple antibodies directed against the core domain of dematin (3). The dematin antibodies used in this study recognized both human and mouse dematin in a comparable fashion, as indicated in our previous studies (1, 10). Immunoblotting of mouse dematin was performed according to the protocol previously developed in our laboratory for mouse fibroblasts (14). Briefly, washed WT and HPKO platelets were treated with the proteasome inhibitors, lactacystin (10 μM) and MG-132 (5 μM), for 30 min at 4 °C. Platelet fractions were then isolated by sonication and centrifugation. The membrane fraction was probed with a dematin polyclonal antibody and a polyclonal β-tubulin antibody from Sigma. Human platelet fractions were isolated using a previously published protocol (19). Platelet fractions were probed with a dematin monoclonal antibody, a PDI monoclonal antibody to detect the dense tubular system (DTS), and a monoclonal antibody against GPIbα to detect the plasma membrane fraction. A monoclonal antibody (sc-100385) against human IP3KB was purchased from Santa Cruz Biotechnology, Inc. (Santa Cruz, CA), and a monoclonal antibody against RhoA was used as a loading control.

Immunofluorescence Analysis—Glass coverslips were coated with 100 μg/ml human fibrinogen in 0.1 M $NaHCO_3$ (pH 8.3) at 4 °C overnight, and wells were blocked with 5% BSA. Washed human platelets (5×10^7 platelets/ml) were added to each well and incubated for 60 min at 37 °C. After washing, platelets were fixed with 4% paraformaldehyde in PBS, treated with the permeabilization buffer (100 mM Tris-HCl, pH 7.4, 10 mM EGTA, 154 mM NaCl, 5 mM $MgCl_2$, 0.5 mM leupeptin, 1.0 mM PMSF, and 0.1% Triton X-100), and blocked with 5% BSA. Dematin monoclonal, PDI monoclonal, and dematin polyclonal antibodies were used with the appropriate secondary antibodies. Finally, the coverslips were mounted to slides, and immunofluorescence images were recorded using a 100× objective on a Nikon TE-2000E inverted microscope.

Measurement of cAMP in Platelets—cAMP measurements were performed using a protocol as described previously (20, 21). Briefly, phosphodiesterase inhibitor Ro 20–1724 (100 μM) was added to WT and HPKO platelets. The platelets were centrifuged, and the pellet fraction was snap frozen in the liquid nitrogen. The platelet pellet was resuspended in 50 mM sodium acetate buffer, sonicated, boiled for 4 min, and then snap frozen to precipitate the proteins. Upon thawing, the samples were centrifuged, and the supernatant was transferred to a new tube to quantify cAMP. A standard curve of cAMP was generated to quantify cAMP levels in the samples. Samples were incubated with [^{3}H]cAMP, PKA inhibitor, and PKA. Potassium phosphate (20 mM) was then added, and samples were filtered to collect the cAMP-PKA complex. Filters were then dissolved with Cellosolve, and radioactivity was measured using a Beckman LS 6500 liquid scintillation counter.

Platelet Spreading Assay—This assay was similar to the immunofluorescence assay with minor modifications. Glass coverslips were coated with 100 μg/ml human fibrinogen in 0.1 M $NaHCO_3$ at 4 °C overnight and then blocked with 5% BSA for

[2] The abbreviations used are: HPKO, headpiece knockout; DKO, double knock-out; DTS, dense tubular system; IP, immunoprecipitation; IP_3, inositol trisphosphate; IP_4, inositol tetraphosphate; IP3KB, inositol 1,4,5-trisphosphate 3-kinase isoform B; PDI, protein-disulfide isomerase; PRP, platelet-rich plasma; TRITC, tetramethylrhodamine isothiocyanate.

90 min. Washed mouse platelets (5×10^7 platelets/ml) were preincubated with DMSO or 10 μM indomethacin and 2.0 units/ml apyrase for 30 min. Platelets were added to each well and allowed to incubate for up to 90 min at 37 °C. The wells were washed and fixed with 4% paraformaldehyde in PBS. Platelets were treated with the permeabilization buffer (100 mM Tris-HCl, pH 7.4, 10 mM EGTA, 154 mM NaCl, 5.0 mM $MgCl_2$, 0.5 mM Leupeptin, 1.0 mM PMSF, and 0.1% Triton X-100) and blocked with 5% BSA. Phalloidin-Alexa 594 at 2.0 μg/ml was added to visualize F-actin. The coverslips were mounted to glass slides and immunofluorescence images were recorded using a ×100 objective on a Nikon TE-2000E microscope. Platelet surface area was calculated using MetaMorph software, and statistical significance was determined using Student's *t* test.

Aggregation and Dense Granule Secretion Measurements—Platelet secretion was measured using the luciferin/luciferase reagent (Chrono-Lume) to detect the release of ATP from platelet dense granules. Platelet aggregation was measured by changes in the light transmission. Mouse washed platelets (2×10^8 platelets/ml) were incubated for 3 min with the Chrono-Lume prior to stimulation. Platelets were treated with a specific agonist at a range of concentrations to establish a dose-response curve. The following agonists were used: 0.6–2.0 μg/ml collagen, 0.25–1.0 μM U46619, 5–10 μM ADP, and 40–100 μM TRAP4 (thrombin receptor-activating peptide 4). All experiments were recorded in real time in a model 700 Chrono-log Lumiaggregometer at 37 °C with stirring (1,000 rpm). Statistical significance was determined using Student's *t* test.

Platelet Fractionation—Platelet fractions were isolated similar to a previously established procedure (19). Briefly, washed human and mouse platelets (2×10^9 platelets/ml) were incubated in lysis buffer (1% Nonidet P-40, 50 mM Tris-HCl, 154 mM NaCl, 1 mM Na_3VO_4, 1 mM EGTA, 1 mM NaF, with protease inhibitors) and centrifuged at 19,000 × *g* for 25 min to remove intact platelets, granules, and mitochondria. The supernatant was centrifuged at 100,000 × *g* for 60 min. The resulting pellet was resuspended and represents the mixed membrane fraction, and the high speed supernatant represents the cytosolic fraction. The two fractions were adjusted to equivalent protein concentrations for Western blotting using a BCA protein assay (Pierce). For additional studies, the fraction containing mixed membranes was layered over a 40% sucrose gradient and centrifuged at 100,000 × *g* for 120 min. The resulting higher density band represents the DTS, and the band at the sucrose interface represents the plasma membrane fraction. The DTS is the primary storage site for intraplatelet releasable calcium. Material in each fraction was washed and recentrifuged before the Western blotting analysis.

Flow Cytometry—Washed WT and HPKO platelets (1×10^8 platelets/ml) were stimulated with an agonist and incubated for 5 min at 37 °C without stirring. Platelets were incubated with reagents conjugated to a fluorophore (P-selectin or JON/A) for 15 min at room temperature under cover. Finally, PBS was added to each sample to terminate the reaction, and samples were immediately analyzed with a FACSCalibur flow cytometer (BD Biosciences) to measure FSC (platelet size), P-selectin expression (α-granule secretion), and JON/A expression (integrin $\alpha_{IIb}\beta_3$ activation). Statistical significance was determined using Student's *t* test.

Clot Retraction—Blood from six WT and six HPKO mice was anticoagulated with 1/10 volume of 3.8% sodium citrate. PRP was isolated by centrifugation of the whole blood at 100 × *g* for 15 min. The platelet count in PRP was adjusted with platelet-poor plasma, and packed erythrocytes were added to enhance the contrast of the clot. After resting for 60 min, 2 mM $CaCl_2$ was added, and the PRP was stimulated with 0.4 unit/ml thrombin and gently mixed. Platelets were allowed to incubate at 37 °C for up to 12 h. Two-dimensional size of the retracted clots was quantified using the NIH ImageJ software, and clot retraction was expressed as the percentage retraction (1 − (final clot size/initial clot size)). Statistical significance was determined using Student's *t* test.

Tail Bleeding Assay—Bleeding time was measured by cutting off the tip (5 mm) of the tail from each WT and HPKO adult (8–12 weeks) mouse. The tail was immediately immersed in PBS at 37 °C. Bleeding time was recorded until the stable cessation of bleeding was observed. Bleeding experiments were terminated after 420 s if the tail bleeding did not stop. Statistical significance was determined using Student's *t* test.

Measurement of Cytoplasmic Ca^{2+} Concentration—Washed platelets (7.5×10^8 platelets/ml) from WT and HPKO mice were resuspended in modified Tyrode's buffer. 15 μM FURA-PE3/AM conjugate (Calbiochem) was added to each sample, and samples were allowed to incubate for 30 min at room temperature in the dark. The samples were centrifuged, and the platelets were resuspended in modified Tyrode's buffer (containing 0.1% BSA) and diluted to 1×10^8 platelets/ml. At this point, 1.0 mM $CaCl_2$, 200 μM EGTA, or 10 μM doxorubicin were added, depending on the experiment. The platelets were loaded onto a 96-well assay plate and incubated for 1 h. The agonists (collagen, U46619, TRAP4, A23187, and Thapsigargin) were added robotically, and the samples were analyzed using a FlexStation II (Molecular Devices). Platelet samples were excited at 340/380 nm, and calcium fluorescence was measured at the emission wavelength of 510 nm. The relative Ca^{2+} fluorescence value was computed by dividing the fluorescence at 340 nm by the fluorescence at 380 nm for each time point. Statistical significance was determined using Student's *t* test.

Proteomics and Immunoprecipitation—Washed platelets were resuspended in lysis buffer, and lysate was incubated on ice for 30 min to promote complete lysis. The cell lysate was centrifuged for 25 min at 15,000 × *g* to remove any intact and aggregated platelets. Immunoprecipitation was performed on the lysates using a cross-link-immunoprecipitation (IP) kit from Pierce. Briefly, the lysate supernatant was precleared with control beads for 1 h to remove any nonspecific interactions. The precleared lysate was incubated with Protein A/G beads cross-linked to dematin monoclonal antibody for 2 h at room temperature. A monoclonal antibody against GAKIN was used as a negative control under the same conditions. The beads were washed, and bound proteins were eluted and analyzed by SDS-PAGE. The gel was stained with colloidal Coomassie Blue, and prominent protein bands were excised and analyzed by mass spectrometry as described previously (1). The presence of dematin in the immunoprecipitate was confirmed by Western

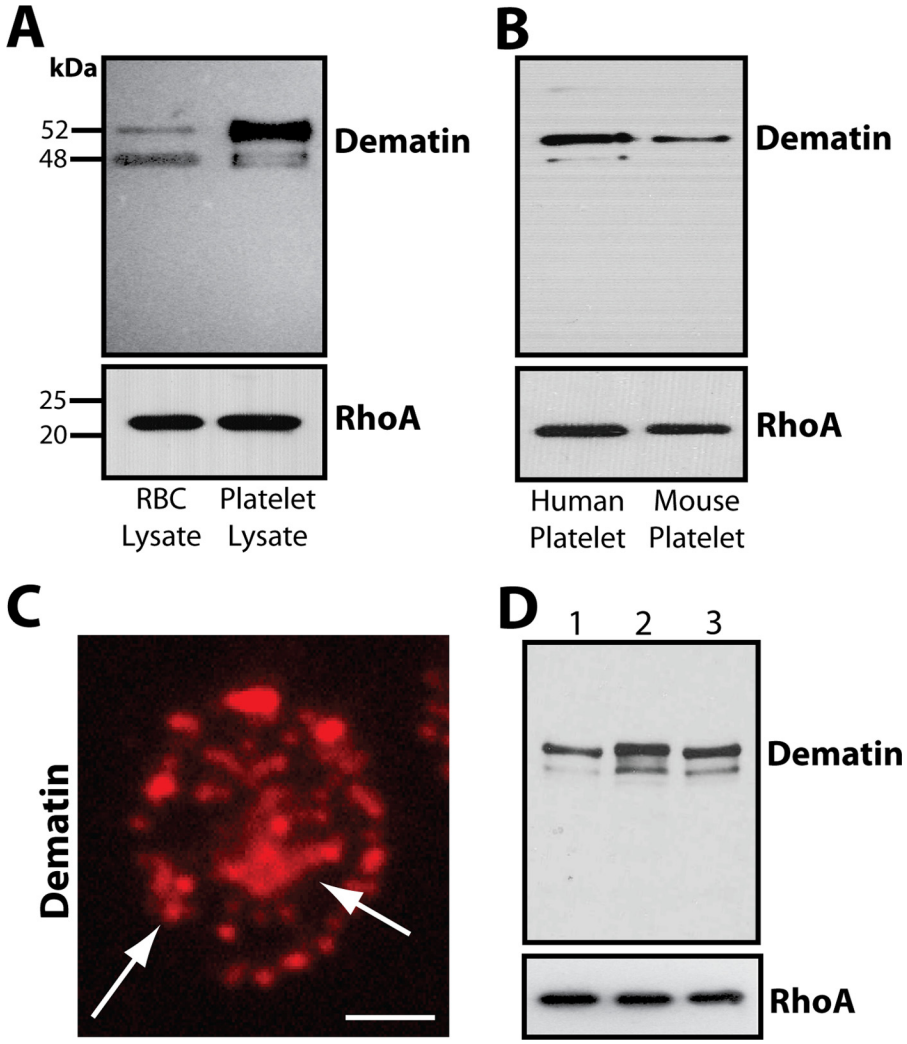

FIGURE 1. **Dematin expression in human and mouse platelets.** *A*, human RBC membrane lysate and human platelet (3×10^8/ml) lysate were analyzed by Western blotting using a dematin-specific monoclonal antibody directed to the core domain. The same material was blotted using an antibody against RhoA. *B*, the larger 52-kDa isoform of dematin is detected both in the human platelet lysate and mouse platelet membrane. The same material was blotted using an antibody against RhoA. *C*, immunofluorescence analysis of dematin in human platelets. Punctate staining pattern of dematin is detected at the membrane as well as in the center of the cell. *Scale bar*, 5 μM. *D*, human platelet lysate (*lane 1*), membrane (*lane 2*), and cytosol fractions (*lane 3*) were normalized for protein and analyzed for relative dematin and RhoA expression by Western blotting.

blotting using a dematin monoclonal antibody and TrueBlot secondary antibody from eBioscience. To detect the dematin-IP3KB complex, platelet lysate was immunoprecipitated with a monoclonal antibody against IP3KB, and dematin in the immunoprecipitate was detected using a monoclonal antibody against dematin and TrueBlot secondary antibody as described above. This biochemical association was confirmed with a reverse co-IP experiment in which dematin immunoprecipitated from human platelet lysates was probed with an IP3KB monoclonal antibody and TrueBlot secondary anti-mouse antibody.

RESULTS

Dematin Is Abundantly Expressed in Platelets—Previous immunoblotting and proteomics studies have indicated the presence of dematin in platelets (13, 22), but its function in platelets has not been investigated. Using a panel of monoclonal and polyclonal antibodies against human and mouse dematin, which have been previously characterized in our laboratory (10, 14), we examined the expression of dematin in platelets by immunoblotting and immunofluorescence assays. Human platelets were solubilized with SDS-sample buffer, and total protein fraction was analyzed by Western blotting using a monoclonal antibody against the core domain of dematin. As compared with human erythrocytes, where the 48-kDa isoform of dematin is dominant (Fig. 1*A*, *left lane*), human platelets predominantly express the 52-kDa isoform of dematin (Fig. 1*A*, *right lane*). A similar expression profile of dematin was observed in both human and mouse platelets (Fig. 1*B*). Quantification of Western blots indicated that the relative expression of dematin in mouse platelets is 40.1% as compared with human platelets (Fig. 1*B*). At higher exposure of Western blots, a faint band of 48 kDa is also detectable in both human and mouse platelets (Fig. 1, *A* and *B*). Using a dematin monoclonal antibody, immunofluorescence analysis confirmed abundant expression of dematin in human platelets (Fig. 1*C*). The subcellular punctate distribution of dematin appears to be concen-

TABLE 1
Platelet analysis of dematin HPKO mice
Data are mean ± S.E. ($n = 5$). MPV, mean platelet volume; MFI, mean fluorescence intensity.

Selected parameters	WT	HPKO
Platelet number (1000/μl)	1416 + 145	1394 + 44
Platelet volume (MPV) (fl)	8.68 ± 0.17	8.8 ± 0.6
Basal cAMP (pmol/10^8) platelets	1.07 ± 0.27	1.17 ± 0.03
Surface expression of integrin $\alpha_{IIb}\beta 3$ (MFI)	28.4 ± 5.2	29.8 ± 3.4

trated at the cell periphery as well as at the center of the platelet (Fig. 1*C*). In addition, biochemical fractionation of human platelets indicated that dematin is associated with both membrane and cytosolic compartments (Fig. 1*D*). Densitometry-based quantification of Western blots indicated that ~68% of dematin is associated with the membrane fraction, whereas ~32% is recovered in the cytosolic fraction of human platelets under resting conditions.

Status of Dematin in HPKO Platelets—The abundant expression of dematin implied a functional role in platelet physiology. To investigate dematin's function in mature platelets, we utilized our HPKO mouse model system (2), where the headpiece domain of dematin was genetically deleted (supplemental Fig. S1*A*). The membrane fraction from WT and HPKO platelets was subjected to Western blotting using an affinity-purified polyclonal antibody against the core domain of mouse dematin. As expected, the mutant dematin protein was truncated in the HPKO platelets as compared with the WT platelets (supplemental Fig. S1*B*). Densitometry analysis indicated ~65% reduction in the expression of truncated dematin in the HPKO platelets as compared with WT platelets (supplemental Fig. S1*C*). These observations suggest either that the truncated core domain of dematin is unstable or that the expression of truncated dematin is reduced in the HPKO mice, and therefore the amount of truncated dematin is significantly reduced in the HPKO platelets. These findings are consistent with our previous observations showing only partial retention of the truncated dematin in the HPKO erythrocyte membranes (2, 10). Further hematological and biochemical analysis of resting platelets indicated no measurable differences in the platelet number, size, volume, basal cAMP level, and integrin $\alpha_{IIb}\beta_3$ expression in the HPKO and WT platelets (Table 1).

HPKO Platelet Spreading on Fibrinogen Matrix—Dematin has been implicated as a modulator of actin dynamics in erythrocytes and fibroblasts (9, 14). This view is consistent with the observation that the headpiece domain of dematin shows sequence similarity to the villin headpiece domain, a known regulator of actin reorganization in response to various stimuli (23). Because of functional similarities in the components of the membrane skeleton between erythrocytes and platelets (17), we investigated the effects of headpiece domain deletion on platelet spreading and actin reorganization. First, platelets from WT and HPKO mice were spread on a fibrinogen-coated surface for 90 min, and platelet spreading was monitored by staining with TRITC-phalloidin to detect F-actin. A measurable defect in platelet spreading was observed in HPKO mice, particularly at the early stages of platelet spreading (Fig. 2*A*). Statistical analysis confirmed that there were significant differences in platelet adherence (Fig. 2*B*) and platelet surface area (Fig. 2*C*) phenotypes of HPKO mice as compared with WT mice. In contrast, when a similar spreading assay was performed using platelets that were treated with the secretory inhibitors apyrase and indomethacin, the HPKO platelets did not show any measurable difference in their ability to spread on the fibrinogen-coated surface as compared with WT controls (supplemental Fig. S2).

HPKO Platelets Exhibit Defective Inside-out Signaling—A platelet spreading phenotype that is dependent upon the release of internal agonists would imply a defect in platelet dense granule secretion (24). Dense granules contain many secretory components, such as ATP, ADP, serotonin, epinephrine, and calcium. We measured ATP release as an index of dense granule secretion and to assess the functional effect of dematin headpiece domain deletion on the platelet secretion process. WT and HPKO platelets were stimulated with multiple agonists (collagen, U46619, and TRAP4), and ATP release was measured using a luciferase assay. The results indicated that dense granule secretion was significantly impaired in the HPKO platelets as compared with WT platelets (Fig. 3). The impaired platelet secretory response was observed at 0.6 μg/ml collagen (Fig. 3*A*), 0.5 μM U46619 (Fig. 3*B*), and 60 μM TRAP4 (Fig. 3*C*). The HPKO platelet secretion defect was partially restored at high concentrations of agonists (Fig. 3*D*). It is to be noted that except for TRAP4, the effect was still significant for all of the other agonists.

α-Granules are secretory organelles responsible for maintaining hemostasis in platelets. They are storage sites for P-selectin, von Willebrand factor, and various clotting proteins (25). We measured the surface expression of P-selectin to determine the effect of dematin headpiece deletion on platelet α-granule secretion. WT and HPKO platelets were stimulated with multiple agonists (collagen, U46619, and TRAP4), incubated with a phycoerythrin-conjugated monoclonal antibody against P-selectin, and flow cytometry was used to quantify P-selectin expression. The results indicated that α-granule secretion was defective in the HPKO platelets. The P-selectin expression response was impaired at 1.0 μg/ml collagen, 0.25 μM U46619, and 60 μM TRAP4 (Fig. 3*E*). Again, increasing the concentration of agonists partially restored the granule secretion defect in HPKO platelets (Fig. 3*E*). These findings suggest that dematin is important for the normal secretion of both α-granules and dense granules in mouse platelets.

Platelet Aggregation Is Reduced in HPKO Mice—Granule secretion is necessary for amplifying the platelet aggregation responses (26). As a consequence, defective granule secretion in the HPKO platelets would suggest a functional abnormality in the platelet aggregation response. To test this prediction, WT and HPKO platelets were stimulated with multiple agonists (collagen, U46619, ADP, and TRAP4), and the platelet aggregation responses were measured by monitoring a change in light transmission upon agonist stimulation. The results indicated that platelet aggregation was inhibited in the HPKO platelets activated by various agonists (Fig. 4). Reduced platelet aggregation was observed at 0.6 μg/ml collagen (Fig. 4*A*), 0.5 μM U46619 (Fig. 4*B*), 10 μM ADP (Fig. 4*C*), and 60 μM TRAP4 (Fig.

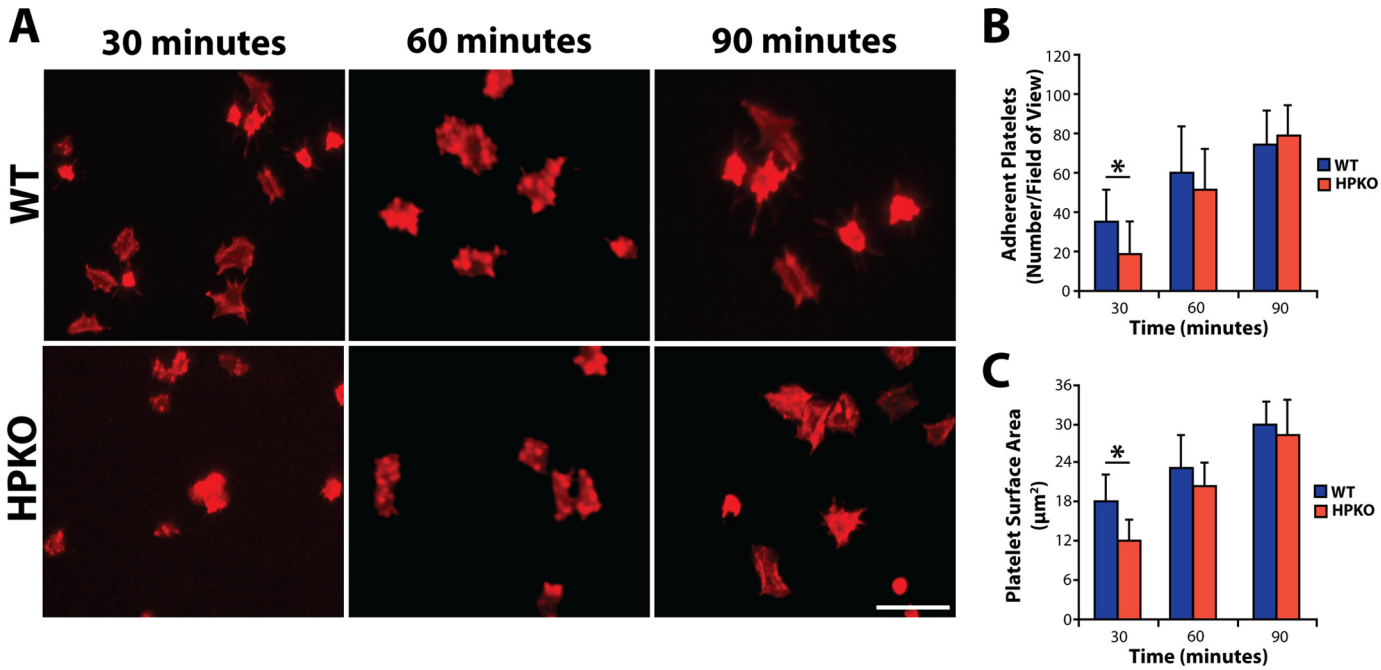

FIGURE 2. **HPKO platelets display abnormal platelet spreading in the absence of secretory inhibitors.** WT and HPKO mouse platelets (5×10^7 platelets/ml) were spread for up to 90 min on the fibrinogen-coated coverslips. *A*, immunofluorescence analysis was performed using Phalloidin-Alexa 594 to detect F-actin. *Scale bar*, 10 μm. Images are representative of three separate experiments. *B*, adhesion was determined by random counts of platelet number per field of view ($n = 10$). *C*, bar graphs display cell surface area (mean ± S.E.) of WT and HPKO platelets using the Metamorph® software. *Error bars*, S.E. from three separate experiments. *, $p < 0.05$.

4*D*). Similar to the secretion response, inhibition of platelet aggregation in the HPKO mice was more prominent at low concentrations of collagen, U46619, and TRAP4 (Fig. 4*E*).

Integrin $\alpha_{IIb}\beta_3$ Activation Is Defective in HPKO Platelets—Impaired platelet secretion and aggregation responses in HPKO mice suggested the existence of additional signaling defects in the mutant platelets. Besides secretion, platelet inside-out signaling exerts a concomitant effect on integrin $\alpha_{IIb}\beta_3$ activation (27). To test this possibility, we examined the status of platelet integrin $\alpha_{IIb}\beta_3$ activation in HPKO mice. WT and HPKO platelets were activated by multiple agonists (collagen, U46619, ADP, and TRAP4) and incubated with the phycoerythrin-conjugated JON/A, an antibody that specifically recognizes the activated form of integrin $\alpha_{IIb}\beta_3$. Integrin activation was measured by flow cytometry, as represented by the mean fluorescence intensity. The results indicated that the activation of integrin $\alpha_{IIb}\beta_3$ is significantly reduced in HPKO platelets in response to multiple agonists (Fig. 4*F*). These observations suggest that dematin plays an important role in platelet inside-out signaling by modulating the cell secretion, aggregation, and integrin $\alpha_{IIb}\beta_3$ activation pathways.

HPKO Mice Show Defects in the Maintenance of Hemostasis—Integrin $\alpha_{IIb}\beta_3$ activation regulates the initiation of outside-in signaling in platelets (28–31). The outside-in signaling pathway in turn regulates the clot retraction and tail bleeding phenotypes. We examined the status of the outside-in signaling pathway in HPKO mice using a clot retraction assay. Platelet-rich plasma from the WT and HPKO mice was stimulated with thrombin (0.4 unit/ml) and allowed to incubate at 37 °C for 12 h (Fig. 5). The clot volume was measured at each time point, and percentage retraction was quantified. The results indicated that the clot retraction was markedly inhibited in the HPKO platelet-rich plasma (Fig. 5*A*). Statistical analysis showed that the clot volume difference was significant at every time point ($p < 0.005$) (Fig. 5*C*). It is known that the addition of $MnCl_2$ can directly activate integrin $\alpha_{IIb}\beta_3$ and thus bypasses integrin activation via the inside-out signaling pathway. Consistent with this model, the addition of $MnCl_2$ rescued the clot retraction defect in HPKO mice (Fig. 5, *B* and *C*). These findings suggest that the clot retraction defect observed in HPKO mice originates from integrin $\alpha_{IIb}\beta_3$ inactivation and is unlikely to be a consequence of defective outside-in signaling in mutant platelets.

Improper platelet-mediated plug formation in the vessel wall leads to impaired hemostasis in mice. Generally, the tail bleeding assay can provide one measure of the *in vivo* hemostatic function. The bleeding assay was performed by cutting the tip of the tail from WT ($n = 40$) and HPKO ($n = 38$) mice and immersing the tip in saline at 37 °C. The time until the stable cessation of bleeding occurred was recorded to determine the mean bleeding time. The HPKO mice displayed slightly longer bleeding times as compared with WT mice (65.2 ± 8.2 s in WT *versus* 73.5 ± 7.6 s in HPKO) (data not shown).

HPKO Platelets Exhibit Defective Intraplatelet Calcium Flux—Previous studies have shown that defects in integrin $\alpha_{IIb}\beta_3$ activation do not necessarily correspond to defects in the platelet secretion pathways (32). Therefore, a possibility existed that dematin may regulate a shared step that is upstream of the two signaling outcomes. Calcium mobilization is one such signaling event that occurs prior to both platelet secretion and integrin $\alpha_{IIb}\beta_3$ activation in platelets (33). In fact, platelet activation by any stimulatory agonist results in the elevation of cytosolic calcium (34). Therefore, calcium release in platelets is vital for the transduction of converging pathways into subsequent inside-

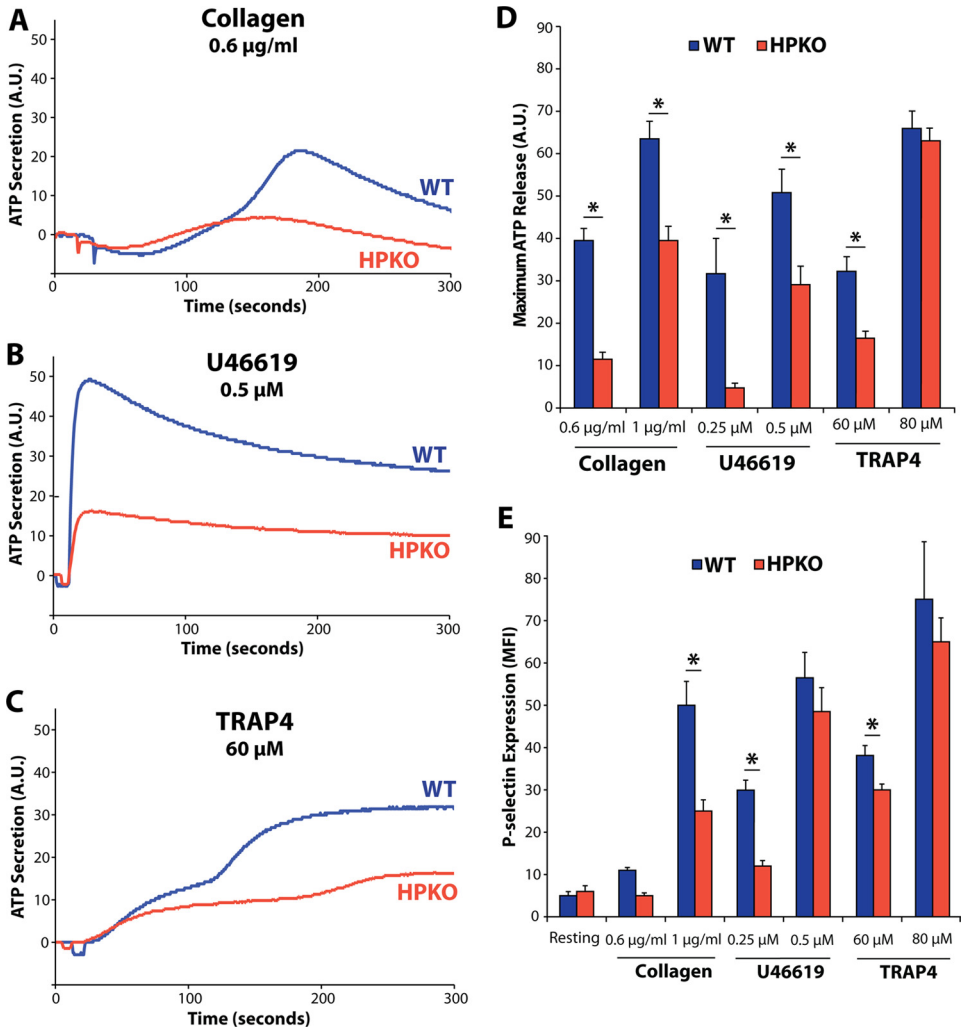

FIGURE 3. **Abnormal platelet secretion in HPKO platelets.** Dense granule secretion was evaluated by measuring the ATP release from WT (*blue*) and HPKO (*red*) platelets induced by 0.6 μg/ml collagen (38.9 $\pm$ 3.9 in WT *versus* 12.1 $\pm$ 1.2 in HPKO, $p < 0.05$) (*A*); 0.5 μM U46619 (51.3 $\pm$ 5.4 in WT *versus* 29.8 $\pm$ 3.3 in HPKO, $p < 0.05$) (*B*); and 60 μM TRAP4 (31.2 $\pm$ 2.9 in WT *versus* 17.5 $\pm$ 1.8 in HPKO, $p < 0.05$) (*C*). *A.U.*, arbitrary units. *D*, the maximum ATP release by three agonists is shown in a histogram. *E*, α-granule secretion was determined by flow cytometry of P-selectin exposure on WT or HPKO platelets. Platelets were activated with collagen (0.6 and 1.0 μg/ml) (for 1.0 μg/ml, the values were 50.0 $\pm$ 5.4 in WT *versus* 23.4 $\pm$ 3.7 in HPKO, $p < 0.05$), U46619 (0.25 and 0.5 μM) (for 0.25 μM U46619, the values were 30.7 $\pm$ 1.8 in WT *versus* 11.9 $\pm$ 1.1 in HPKO, $p < 0.05$), or TRAP4 (60 and 80 μM) (for 60 μM TRAP4, the values were 38.1 $\pm$ 2.9 *versus* 30.5 $\pm$ 1.8 in HPKO, $p < 0.05$) and labeled with FITC-labeled anti-P-selectin mAb. The level of P-selectin exposed on the surface of platelets is expressed as mean fluorescence intensity (*MFI*). *Error bars*, S.E. from three separate experiments.

out signaling events. To investigate this possibility, we examined the status of calcium signaling response in HPKO platelets. Washed platelets in the presence of 1.0 mM $CaCl_2$ were labeled with FURA-PE3/AM, a cytosolic calcium-sensitive dye, and platelets were activated by various agonists (collagen, U46619, TRAP4, ADP, and A23187). Calcium fluorescence measurements indicated that there was a significant defect in calcium mobilization upon agonist stimulation in HPKO platelets (Fig. 6). As an internal control, the addition of calcium ionophore, A23187, induced an equal and complete response in both WT and HPKO platelets (Fig. 6*E*). The calcium mobilization defect in HPKO platelets was somewhat tempered as the concentration of agonists was raised (Fig. 6*F*).

HPKO Platelets Show Impaired Intraplatelet Calcium Release—An imbalance in the total calcium flux can originate either from the impaired influx of extracellular calcium through the platelet plasma membrane or from the inhibition of calcium release from the internal platelet stores. Therefore, by removing the extracellular calcium from the medium, the only detectable cellular calcium will be released from the intraplatelet pool. To test this possibility, a calcium mobilization assay was performed in WT and HPKO platelets by omitting the calcium in the Tyrode's buffer. For this assay, TRAP4 and U46619 were used to exert the agonist-induced calcium release in platelets. The HPKO platelets exhibited a significant defect in the calcium mobilization upon stimulation by agonists (Fig. 7). The calcium mobilization defect was observed by stimulation with 0.5 μM U46619 (Fig. 7*A*) and 60 μM TRAP4 (Fig. 7*B*). Calcium release in platelets was also stimulated with Thapsigargin, an inhibitor of SERCA (sarco/endoplasmic reticulum calcium ATPase). Thapsigargin causes the depletion of calcium from internal stores, including the DTS. Using 200 nM Thapsigargin, the targeted release of calcium from the DTS was also defective in HPKO platelets (Fig. 7*C*). The defect in the release of intracellular calcium was observed at multiple doses of each agonist in HPKO platelets (Fig. 7*D*). These results indicate that

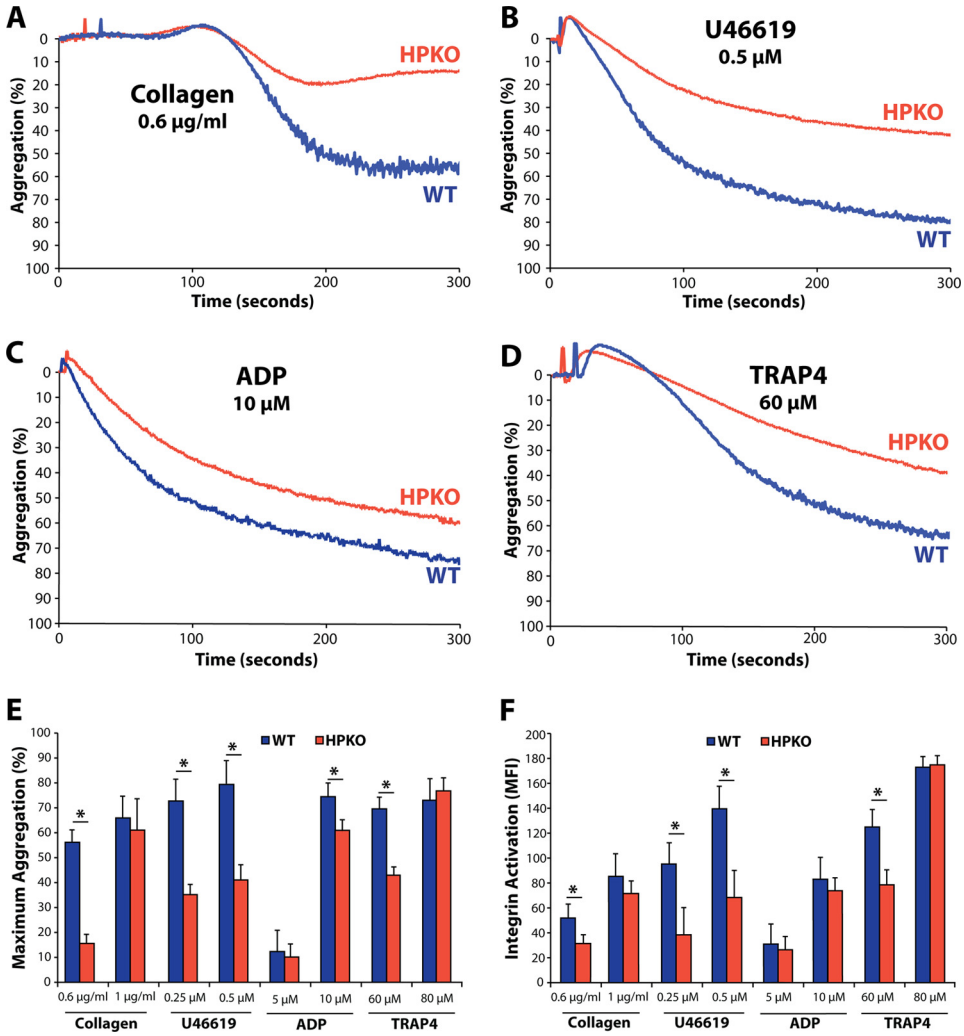

FIGURE 4. **Aggregation response and integrin activation in HPKO platelets.** To assess the status of inside-out signaling, WT (*blue*) and HPKO (*red*) platelets were analyzed for aggregation response to 0.6 μg/ml collagen (56.2 $\pm$ 6.2% in WT *versus* 15.5 $\pm$ 4.1% in HPKO, $p < 0.05$) (*A*), 0.5 μM U46619 (79.8 $\pm$ 10.0% in WT *versus* 41.2 $\pm$ 5.3% in HPKO, $p < 0.05$) (*B*), 10 μM ADP (75.3 $\pm$ 4.7% in WT *versus* 60.8 $\pm$ 4.5% in HPKO, $p < 0.05$) (*C*), and 60 μM TRAP4 (69.8 $\pm$ 4.6% in WT *versus* 43.3 $\pm$ 3.8% in HPKO, $p < 0.05$) (*D*). *E*, data for maximum aggregation are shown in the histogram. *F*, integrin $\alpha_{IIb}\beta_3$ activation was assessed by flow cytometry of WT and HPKO platelets. Platelets were activated by collagen (0.6 or 1.0 μg/ml) (0.6 μg/ml collagen: 51.2 $\pm$ 12.8 in WT *versus* 31.1 $\pm$ 8.5 in HPKO, $p < 0.05$), U46619 (0.25 or 0.5 μM) (0.25 μM U46619: 98.4 $\pm$ 17.7 in WT *versus* 38.8 $\pm$ 20.9 in HPKO, $p < 0.05$), ADP (5 or 10 μM), and TRAP4 (60 or 80 μM) (60 μM TRAP4: 125.3 $\pm$ 13.6 in WT *versus* 79.1 $\pm$ 10.3 in HPKO, $p < 0.05$). Phycoerythrin-labeled anti-integrin $\alpha_{IIb}\beta_3$ mAb (JON/A) was used to specifically detect the activated conformation of mouse integrin $\alpha_{IIb}\beta_3$. *Error bars*, S.E. from three separate experiments.

the dematin headpiece domain regulates the flux of calcium across the dense tubular system in mouse platelets.

Dematin Is Located at the DTS in Platelets—As indicated before, immunofluorescence analysis identified a fraction of dematin concentrated at an unidentified central region in platelets (Fig. 1*C*). Because calcium release from the DTS appeared to be defective in the HPKO platelets (Fig. 6), the localization of dematin was evaluated relative to DTS in platelets. Human platelets were examined with a monoclonal antibody to detect the endogenous dematin and a polyclonal antibody to detect the PDI. PDI has been shown to concentrate predominantly in the platelet DTS (35). Immunofluorescence analysis indicated a clear overlap between a fraction of dematin and PDI in human platelets (Fig. 8*A*). Although a substantial portion of total dematin is also detected at other sites in platelets, most notably the plasma membrane, the PDI co-localization data suggest that a significant fraction of dematin is located at the DTS in human platelets. To further confirm this observation, human platelets were biochemically fractionated into plasma membrane and intracellular membrane (DTS) fractions. Western blot analysis indicated that a significant amount of dematin is recovered in the fraction containing intracellular membranes, thus further lending support to the co-localization of dematin with PDI in platelets (Fig. 8*B*). It is of note that a slight change in the molecular mass of dematin in the plasma and intracellular membranes is likely to be due to the differential propensity of disulfide bond formation of dematin polypeptides, thus resulting in dimeric or higher oligomeric species, as is the case with erythrocyte dematin (2).

Dematin-associated Proteins at the DTS in Platelets—To further investigate the mechanisms that give rise to reduced calcium mobilization in dematin HPKO platelets, we performed IP of dematin from platelets and identified dematin-associated proteins by mass spectrometry. It is to be noted that an IP of dematin in platelets poses unique technical challenges because of the tight association of dematin with the membrane fraction.

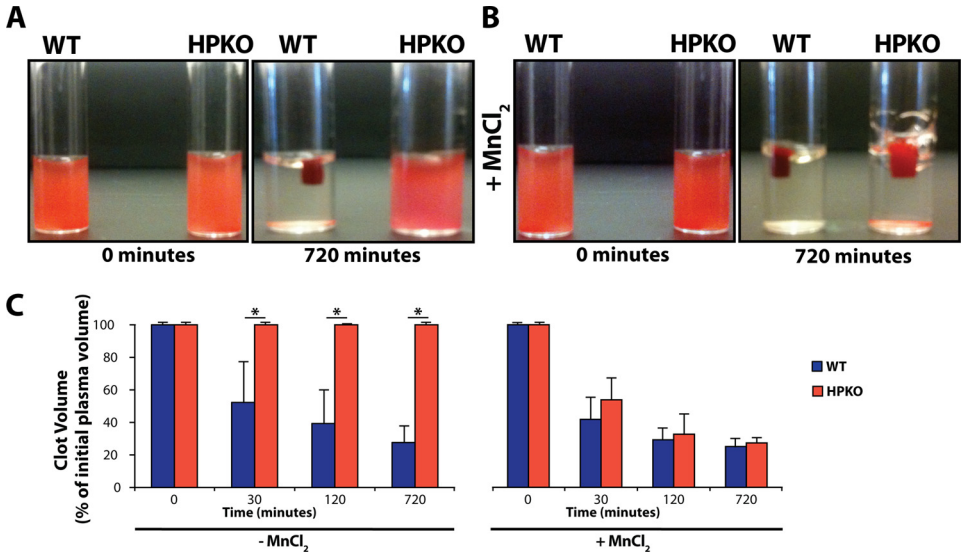

FIGURE 5. **HPKO mice display features of unstable thrombosis.** *A*, clot retraction phenotype of WT and HPKO mice. Platelet-rich plasma was incubated at 37 °C with thrombin (0.4 unit/ml) for 720 min. *B*, 0.5 mM $MnCl_2$ was added prior to the addition of thrombin to activate integrin $\alpha_{IIb}\beta_3$ receptor. *C*, the clot volume of each time point is plotted in a histogram. *Error bars*, S.E. from three separate experiments.

The disruption of the dematin biochemical complex under harsh conditions and its reassociation under mild detergent conditions may prevent identification of some physiologically relevant interactions by this approach. This is one reason why the dematin-binding proteins in erythrocytes were not identified by conventional immunoprecipitation and proteomics approaches. Nonetheless, suitable biochemical conditions were optimized to immunoprecipitate dematin-associated proteins in platelets. Proteomics analysis of the dematin immunoprecipitated proteins revealed several calcium-sensitive proteins that could be potentially associated with the DTS in platelets and contribute to the release of calcium. These proteins include protein-disulfide isomerase A5, IP3KB, caldesmon, and calmodulin-like protein 5. Of these candidate proteins, only IP3KB has been shown to directly regulate calcium release in cells (36, 37). IP3KB functions to phosphorylate IP_3 into IP_4, thereby eliminating the ability of IP_3 to activate the IP_3 receptor and liberate calcium from intracellular pools (38). To validate our proteomics findings, we performed immunoprecipitation analysis using antibodies against IPK3B and dematin in platelets. The results demonstrate that both dematin and IPK3B exist in the same biochemical complex in human platelets (Fig. 8, *C* and *D*).

Loss of the dematin headpiece in mouse platelets results in a significant decrease of IP3KB detected in the platelet membrane fraction (Fig. 8*E*). The reduced level of IP3KB at the membrane translates to an increase in liberated IP3KB detected within the cytosol in the HPKO platelets (Fig. 8*E*). Furthermore, by utilizing doxorubicin, a known inhibitor of IP3KB (39, 40) and calcium release in platelets (41), a significant rescue was demonstrated in the HPKO intraplatelet calcium release (Fig. 8*F*). With the biochemical and mechanistic validation of the dematin-IP3KB complex in platelets, we propose that this novel interaction may offer a mechanism for the modulation of intraplatelet calcium by dematin, with broad implications in cells where both dematin and IP3KB are abundantly expressed.

DISCUSSION

The spectrin-based membrane skeleton in erythrocytes has served as a paradigm for cytoskeletal organization in many nonerythroid cells, including platelets (17, 42). For example, adducin, a component of the erythrocyte spectrin-actin junctions where dematin is also located, plays an important role in the reorganization of the membrane cytoskeleton in platelets (17, 43). Our recent studies have shown a compensatory role of dematin and adducin in the regulation of erythrocyte shape and membrane properties (10). The present study was initiated to investigate the functional role of dematin in circulating platelets. Western blotting indicated that dematin is abundantly expressed in both human and mouse platelets, and dematin migrates predominantly as a 52-kDa polypeptide on SDS-gel electrophoresis (Fig. 1). Immunofluorescence analysis revealed a distinct punctate pattern of dematin in platelets, and biochemical fractionation assays indicated the location of dematin in both plasma membrane and cytosol fractions (Fig. 1). The abundant expression and localization pattern of dematin suggested that it may regulate key platelet functions. In this paper, we provide the first comprehensive characterization of dematin function in platelets. Our results demonstrate a novel function of dematin in the regulation of calcium flux in platelets stimulated by a variety of physiological agonists, thus placing dematin as a key modulator of platelet secretion and activation pathways.

The generation of dematin HPKO mice in our laboratory (2) enabled us to use this experimental tool to investigate dematin function in platelets. Consistent with our previous findings on HPKO erythrocytes, the HPKO platelets also express a truncated form of dematin encoded by its core domain. A marked reduction of truncated dematin in the HPKO platelets indicates that the deletion of the headpiece domain causes instability of the protein, thus resulting in further degradation of the remaining core domain (supplemental Fig. S1). An alternate explana-

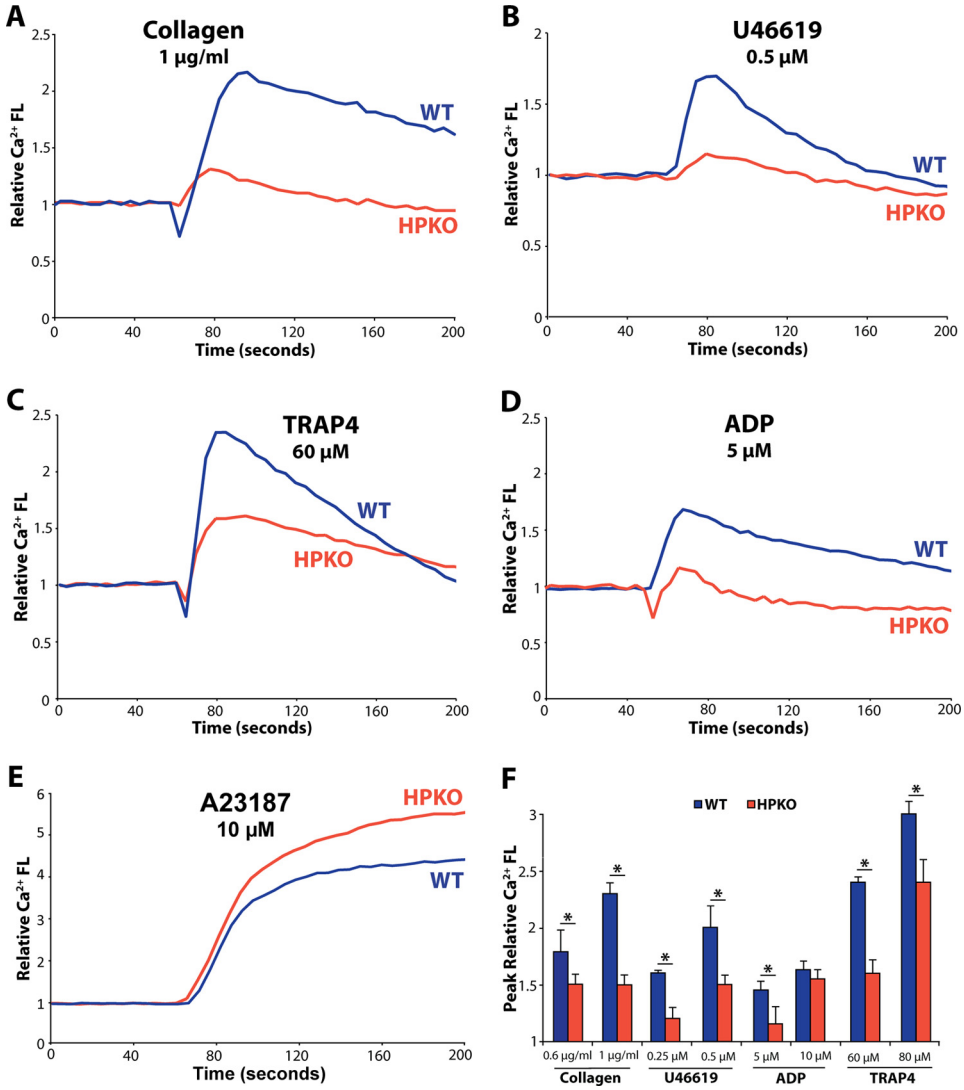

FIGURE 6. **HPKO platelets show a significant defect in total calcium flux.** WT (*blue*) and HPKO (*red*) washed platelets in the presence of 1.0 mM $CaCl_2$ were analyzed for calcium mobilization in response to 1.0 μg/ml collagen (2.31 ± 0.76 in WT *versus* 1.52 ± 0.72 in HPKO, $p < 0.05$) (*A*), 0.5 μM U46619 (2.13 ± 0.22 in WT *versus* 1.61 ± 0.21 in HPKO, $p < 0.05$) (*B*), 60 μM TRAP4 (2.42 ± 0.13 in WT *versus* 1.61 ± 0.22 in HPKO, $p < 0.05$) (*C*), and 5 μM ADP (1.51 ± 0.12 in WT *versus* 1.13 ± 0.21 in HPKO, $p < 0.05$) (*D*). *E*, as an internal positive control, the addition of 10 μM calcium ionophore A23187 induced an equal and complete response in both WT and HPKO platelets. The values reflect relative calcium fluorescence (*FL*). *F*, peak relative calcium fluorescence is plotted, displaying a range of agonist concentrations. *Error bars*, S.E. from three separate experiments.

tion could also involve reduced synthesis and membrane association of truncated dematin during platelet development. In the HPKO mice, the resting platelet morphology and number are not affected, suggesting that dematin does not affect platelet biogenesis and other basal parameters, such as the cAMP level and integrin $\alpha_{IIb}\beta_3$ expression (Table 1). Functionally, the HPKO platelets exhibited a minor defect in platelet spreading, including surface area and adhesion parameters, on fibrinogen at the early stages of platelet spreading (Fig. 2). Interestingly, the HPKO platelets did not display any measurable spreading defects in the presence of known secretion inhibitors (supplemental Fig. S2). This finding suggested a functional role of dematin in the regulation of the platelet secretory pathway. Consistent with this hypothesis, both α-granule and dense granule secretion pathways are attenuated in HPKO platelets when stimulated by multiple agonists, indicating that dematin functions as a key regulator of the secretory process in mouse platelets (Fig. 3).

A defect in the granule secretion pathway would also imply a functional abnormality in the second wave of platelet aggregation phenotype, a step that is dependent upon platelet secretion. Because the HPKO platelets showed aggregation defects at low doses of multiple agonists (Fig. 4), it appears that dematin's involvement in the platelet aggregation pathways is driven largely by its functional role in the dense granule secretion (Fig. 4). A similar linkage may also exist between the platelet secretion and integrin activation in HPKO platelets. Although the basal expression of integrin $\alpha_{IIb}\beta_3$ is unaltered in HPKO platelets, integrin $\alpha_{IIb}\beta_3$ activation is attenuated in the HPKO platelets simulated with multiple agonists (Fig. 4). These findings predicted that attenuated integrin $\alpha_{IIb}\beta_3$ activation may influence other outside-in signaling processes, such as the clot retraction phenotype. This prediction is consistent with the delayed clot retraction phenotype observed in the HPKO mice, which was rescued by the addition of $MnCl_2$ (Fig. 5). In addition, the tail bleeding time is also slightly increased in the

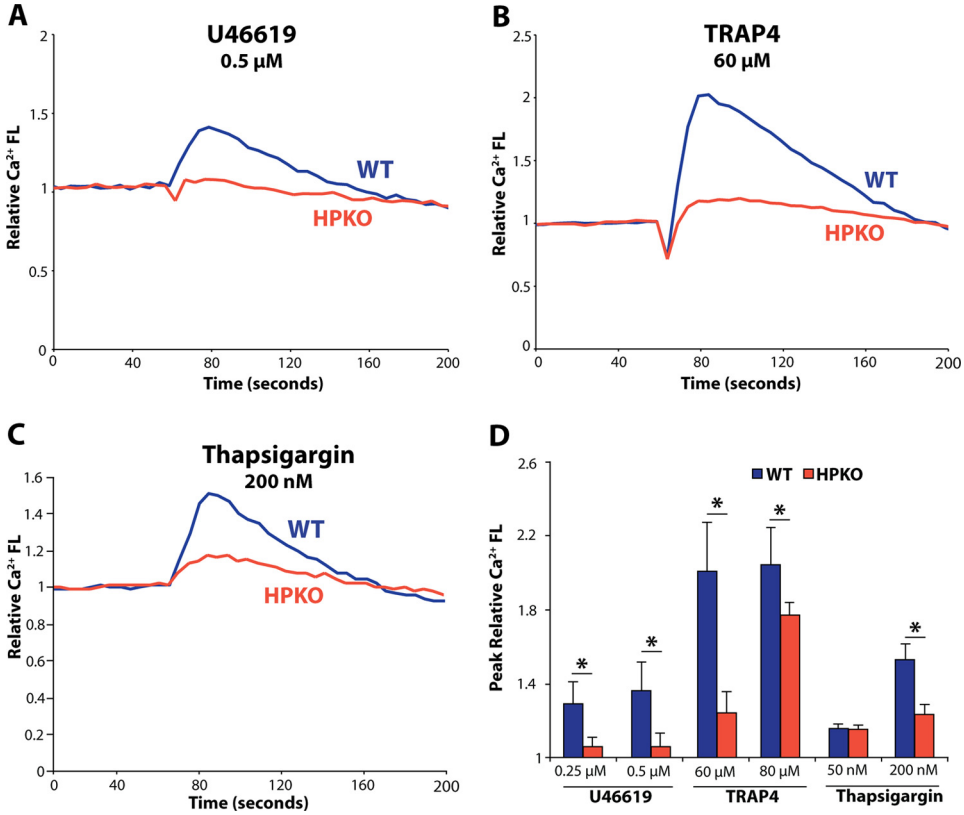

FIGURE 7. **HPKO platelets show a significant defect in internal calcium release.** The effect of the removal of extracellular calcium was investigated using 0.5 μM U46619 (1.38 ± 0.19 in WT *versus* 1.10 ± 0.13 in HPKO) (*A*), 60 μM TRAP4 (1.99 ± 0.32 in WT *versus* 1.21 ± 0.09 in HPKO) (*B*), and 200 nM Thapsigargin (1.52 ± 0.71 in WT *versus* 1.28 ± 0.18 in HPKO; $p < 0.05$) (*C*). *D*, peak relative calcium fluorescence is plotted for various agonists. *Error bars*, S.E. from three separate experiments.

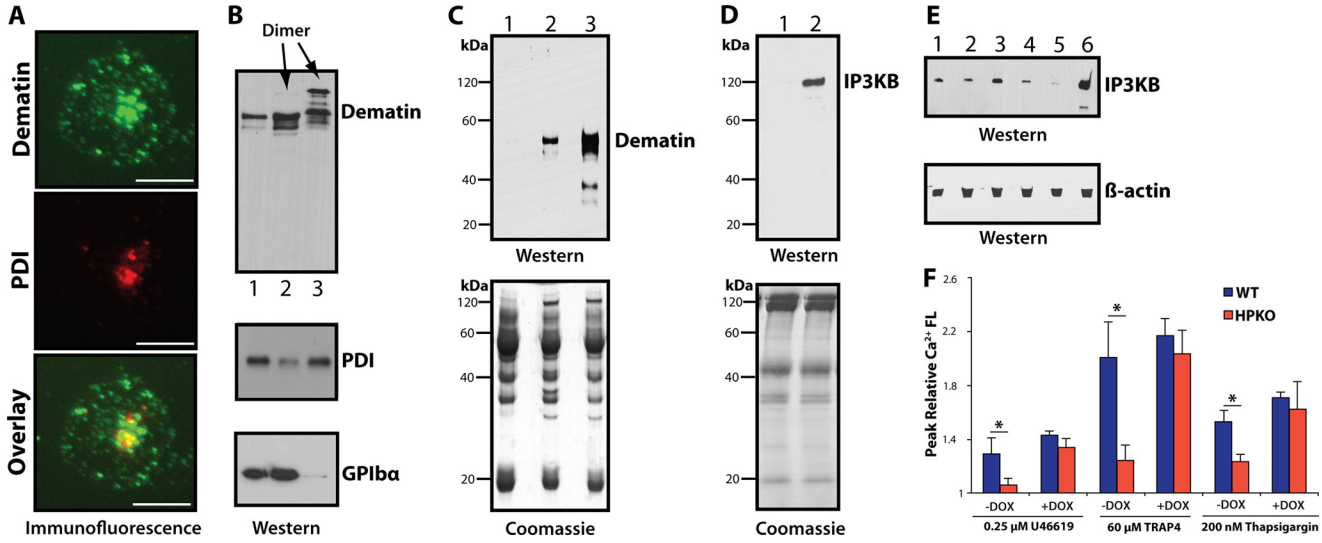

FIGURE 8. **Dematin is located at the plasma membrane and DTS in platelets.** *A*, co-localization analysis was performed using dematin (*green*) and PDI (*red*), a marker of the DTS in platelets. *Scale bar*, 5 μm. *B*, human platelets were washed and fractionated. *Lane 1*, total platelet membranes; *lane 2*, plasma membrane; *lane 3*, intracellular membranes. Each fraction (20 μg of protein) was probed with antibodies against dematin, PDI (to detect DTS), and GPIbα (to detect plasma membrane). A significant expression of dematin was detected in the intracellular membranes. A slight mobility shift of dematin may indicate a post-translational modification. *C*, dematin Western blotting of endogenous co-IP of dematin and IP3KB in human platelets. *Lane 1*, co-IP with an unrelated monoclonal antibody, GAKIN; *lane 2*, co-IP with IP3KB monoclonal antibody; *lane 3*, precleared lysate. The same material was detected by Coomassie Blue after SDS-PAGE. *D*, IP3KB Western blotting of endogenous co-IP of dematin and IP3KB in human platelets. *Lane 1*, co-IP with an unrelated monoclonal antibody, GAKIN; *lane 2*, co-IP with dematin monoclonal antibody. The same material was detected by Coomassie Blue after SDS-PAGE. *E*, IP3KB expression in WT and HPKO platelet fractions. *Lane 1*, total WT platelet lysate; *lane 2*, total HPKO platelet lysate; *lane 3*, WT membrane fractions; *lane 4*, HPKO membrane fractions; *lane 5*, WT cytosolic fraction; *lane 6*, HPKO cytosolic fraction. Each fraction (6 μg of protein) was probed with antibodies against IP3KB and β-actin (control). *F*, the effect of IP3KB inhibition by doxorubicin (*DOX*) on internal calcium release was investigated in WT and HPKO platelets. Peak relative calcium fluorescence is plotted for various agonists with or without 10 μM doxorubicin. *Error bars*, S.E. from three separate experiments.

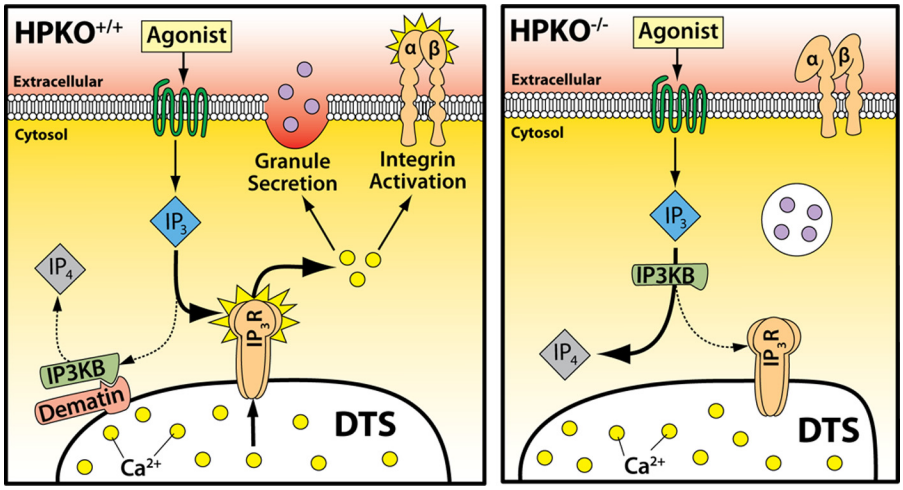

FIGURE 9. **Role of dematin in the calcium mobilization in platelets.** A proposed model for the function of dematin in the platelet signaling cascade. The model predicts that dematin regulates the release of internal calcium at the DTS through a biochemical interaction with IP3KB. Regulation of intracellular calcium release would impact multiple downstream signaling events, including granule secretion and integrin $\alpha_{IIb}\beta_3$ activation.

HPKO mice. The nearly complete recovery of the striking defect in clot retraction by directly activating integrin $\alpha_{IIb}\beta_3$ suggests that there are no major defects in the outside-in signaling pathway in HPKO platelets. Thus, the existence of multiple defects in the secretion, aggregation, and integrin $\alpha_{IIb}\beta_3$ activation pathways places dematin at a central node of the inside-out signaling cascade in platelets.

One mechanism that could potentially explain the pleiotropic effects of dematin headpiece domain deletion in platelets may involve the regulation of intracellular calcium. In platelets, calcium regulation involves the mobilization of intracellular calcium between the DTS and the cytosol as well as the influx of extracellular calcium through the platelet plasma membrane (44–49). In activated platelets, calcium mobilization triggers granule secretion (50), a critical step for regulating key effector molecules that amplify and stabilize the platelet thrombi at the site of vascular injury (51). In platelets, the secretory components are contained within two principal pools: the dense granules and α-granules. The dense granules contain small effector molecules, such as ADP, potentiating platelet activation, whereas the α-granules are storage sites for proteins, such as P-selectin and von Willebrand factor, necessary for hemostasis (51, 52). Our finding showing a marked reduction in the mobilization of intracellular calcium in HPKO platelets, stimulated by multiple agonists, is consistent with the model in which a secretion defect exists in the HPKO platelets. Because the calcium mobilization defect is independent of the level of calcium in the extracellular medium (Fig. 7), our findings suggest that the calcium mobilization defect in HPKO platelets originates from the release of calcium from the intracellular stores in platelets.

The co-localization of dematin with a DTS marker provides further evidence that a significant fraction of dematin is located at the DTS, a key site for the regulation of intracellular calcium release in platelets. By utilizing immunoprecipitation and proteomics techniques, we identified a biochemical association between dematin and IP3KB in platelets (Fig. 8). Furthermore, the proposed mechanism was validated by inhibiting the IP3KB in HPKO platelets and thereby ameliorating the calcium mobilization defect (Fig. 8*F*). IP3KB is a major regulator of calcium homeostasis and is localized at the cytoplasmic face of the endoplasmic reticulum membrane, a counterpart of the DTS in platelets (38). Like dematin, IP3KB is ubiquitously expressed and was recently shown to be enriched within the cortical actin filaments (53). It has been suggested that the localization of IP3KB may offer a means to regulate IP_3 levels in the cells (36, 54). However, the precise mechanism of IP3KB localization at the membrane sites via cortical actin structures is not known (53). Our findings offer one potential mechanism for the cytoskeletal anchor of IP3KB not only in platelets but also in many other cell types. Interestingly, the internal calcium release is not completely ablated in the HPKO platelets (Fig. 6). Therefore, either the residual core domain of dematin provides a low level of calcium release activity or there is a compensatory mechanism for calcium release in the absence of the dematin headpiece domain in mouse platelets. These questions will be addressable in future using platelets completely deficient in full-length dematin.

To integrate our findings, we propose a model illustrating a critical role of dematin in the mobilization of calcium at the DTS of platelets (Fig. 9). Upon agonist stimulation, receptor activation results in the PLC activation, thus leading to the cleavage of PIP_2 into IP_3 and diacylglycerol in platelets. The IP_3 then activates the IP_3 receptor located at the DTS and induces the release of calcium into the cytosol. The liberated calcium then activates many important downstream signaling events, such as the integrin $\alpha_{IIb}\beta_3$ activation, granule secretion, and platelet aggregation. Our model predicts that dematin tightly regulates the localization of IP3KB, a terminator of calcium signaling, via the phosphorylation of IP_3 into IP_4. The cytoskeletal tethering of IP3KB to the DTS prevents unwanted and premature phosphorylation of IP_3, thus maintaining calcium mobilization in platelets (38). Other alternate mechanisms may also entail regulation of dematin-IP3KB interactions by phosphorylation and calpain-mediated proteolysis in activated platelets.

Pathological conditions of platelet dysfunction contribute to the progression of cardiovascular disease, heart attacks, and

stroke (55). Specifically, aberrant calcium signaling in platelets has been reported in diabetic and hypertensive individuals and may be a factor in their disease progression (56, 57). The precise details of the molecular mechanisms of how dematin positively regulates calcium release from the DTS in platelets remain to be elucidated. In erythrocytes, dematin is an excellent substrate of calpain-1, and its phosphorylation by cAMP-dependent protein kinase regulates its association with the actin filaments. Whether these post-translational modifications modulate the function of dematin in platelets remains to be determined. Because dematin is expressed in many non-erythroid tissues, including heart, brain, kidney, and skeletal muscle, it would be important to determine whether dematin performs a similar function regulating calcium homeostasis in these tissues. This study provides the first evidence that dematin functions as a novel regulator of internal calcium release in platelets and plays an important role in the regulation of multiple platelet functions. These findings are likely to provide new insights into the modulation of calcium mobilization and regulation of platelet functions *in vivo*. In conclusion, future characterization of dematin and its signaling pathways by cell-permeable peptides and small molecules may represent a potential therapeutic option for the management of cardiovascular disease and stroke.

Acknowledgments—We are grateful to Drs. David Speicher (Wistar Institute, Philadelphia), for performing the proteomics of dematin-associated proteins in platelets, Jaehyung (Gus) Cho (University of Illinois, Chicago, IL) for sharing the monoclonal antibody against PDI, Subhashini Srinivasan (University of Illinois) for technical advice and assistance in the platelet cAMP measurements, and Xiaoping Du (University of Illinois) for technical advice on platelet activation and secretion experiments. We also thank Donna-Marie Mironchuk (Tufts University) for help with the graphic arts, proofreading, and other technical assistance.

REFERENCES

1. Khan, A. A., Hanada, T., Mohseni, M., Jeong, J. J., Zeng, L., Gaetani, M., Li, D., Reed, B. C., Speicher, D. W., and Chishti, A. H. (2008) Dematin and adducin provide a novel link between the spectrin cytoskeleton and human erythrocyte membrane by directly interacting with glucose transporter-1. *J. Biol. Chem.* **283,** 14600–14609
2. Khanna, R., Chang, S. H., Andrabi, S., Azam, M., Kim, A., Rivera, A., Brugnara, C., Low, P. S., Liu, S. C., and Chishti, A. H. (2002) Headpiece domain of dematin is required for the stability of the erythrocyte membrane. *Proc. Natl. Acad. Sci. U.S.A.* **99,** 6637–6642
3. Husain-Chishti, A., Levin, A., and Branton, D. (1988) Abolition of actin-bundling by phosphorylation of human erythrocyte protein 4.9. *Nature* **334,** 718–721
4. Husain-Chishti, A., Faquin, W., Wu, C. C., and Branton, D. (1989) Purification of erythrocyte dematin (protein 4.9) reveals an endogenous protein kinase that modulates actin-bundling activity. *J. Biol. Chem.* **264,** 8985–8991
5. Roof, D. J., Hayes, A., Adamian, M., Chishti, A. H., and Li, T. (1997) Molecular characterization of abLIM, a novel actin-binding and double zinc finger protein. *J. Cell Biol.* **138,** 575–588
6. Chen, L., Jiang, Z. G., Khan, A. A., Chishti, A. H., and McKnight, C. J. (2009) Dematin exhibits a natively unfolded core domain and an independently folded headpiece domain. *Protein Sci.* **18,** 629–636
7. Frank, B. S., Vardar, D., Chishti, A. H., and McKnight, C. J. (2004) The NMR structure of dematin headpiece reveals a dynamic loop that is conformationally altered upon phosphorylation at a distal site. *J. Biol. Chem.* **279,** 7909–7916
8. Siegel, D. L., and Branton, D. (1985) Partial purification and characterization of an actin-bundling protein, band 4.9, from human erythrocytes. *J. Cell Biol.* **100,** 775–785
9. Azim, A. C., Knoll, J. H., Beggs, A. H., and Chishti, A. H. (1995) Isoform cloning, actin binding, and chromosomal localization of human erythroid dematin, a member of the villin superfamily. *J. Biol. Chem.* **270,** 17407–17413
10. Chen, H., Khan, A. A., Liu, F., Gilligan, D. M., Peters, L. L., Messick, J., Haschek-Hock, W. M., Li, X., Ostafin, A. E., and Chishti, A. H. (2007) Combined deletion of mouse dematin-headpiece and β-adducin exerts a novel effect on the spectrin-actin junctions leading to erythrocyte fragility and hemolytic anemia. *J. Biol. Chem.* **282,** 4124–4135
11. Derick, L. H., Liu, S. C., Chishti, A. H., and Palek, J. (1992) Protein immunolocalization in the spread erythrocyte membrane skeleton. *Eur. J. Cell Biol.* **57,** 317–320
12. Bruce, L. J., Beckmann, R., Ribeiro, M. L., Peters, L. L., Chasis, J. A., Delaunay, J., Mohandas, N., Anstee, D. J., and Tanner, M. J. (2003) A band 3-based macrocomplex of integral and peripheral proteins in the RBC membrane. *Blood* **101,** 4180–4188
13. Faquin, W. C., Husain, A., Hung, J., and Branton, D. (1988) An immunoreactive form of erythrocyte protein 4.9 is present in non-erythroid cells. *Eur. J. Cell Biol.* **46,** 168–175
14. Mohseni, M., and Chishti, A. H. (2008) The headpiece domain of dematin regulates cell shape, motility, and wound healing by modulating RhoA activation. *Mol. Cell. Biol.* **28,** 4712–4718
15. Mohseni, M., and Chishti, A. H. (2009) Regulatory models of RhoA suppression by dematin, a cytoskeletal adaptor protein. *Cell Adh. Migr.* **3,** 191–194
16. Barrientos, T., Frank, D., Kuwahara, K., Bezprozvannaya, S., Pipes, G. C., Bassel-Duby, R., Richardson, J. A., Katus, H. A., Olson, E. N., and Frey, N. (2007) Two novel members of the ABLIM protein family, ABLIM-2 and -3, associate with STARS and directly bind F-actin. *J. Biol. Chem.* **282,** 8393–8403
17. Barkalow, K. L., Italiano, J. E., Jr., Chou, D. E., Matsuoka, Y., Bennett, V., and Hartwig, J. H. (2003) α-Adducin dissociates from F-actin and spectrin during platelet activation. *J. Cell Biol.* **161,** 557–570
18. Leng, L., Kashiwagi, H., Ren, X. D., and Shattil, S. J. (1998) RhoA and the function of platelet integrin αIIbβ3. *Blood* **91,** 4206–4215
19. Kovàcs, T., Berger, G., Corvazier, E., Pàszty, K., Brown, A., Bobe, R., Papp, B., Wuytack, F., Cramer, E. M., and Enouf, J. (1997) Immunolocalization of the multi-sarco/endoplasmic reticulum Ca^{2+} ATPase system in human platelets. *Br. J. Haematol.* **97,** 192–203
20. Gilman, A. G. (1970) A protein binding assay for adenosine 3′:5′-cyclic monophosphate. *Proc. Natl. Acad. Sci. U.S.A.* **67,** 305–312
21. Srinivasan, S., Mir, F., Huang, J. S., Khasawneh, F. T., Lam, S. C., and Le Breton, G. C. (2009) The P2Y12 antagonists, 2-methylthioadenosine 5′-monophosphate triethylammonium salt and cangrelor (ARC69931MX), can inhibit human platelet aggregation through a G_i-independent increase in cAMP levels. *J. Biol. Chem.* **284,** 16108–16117
22. Zahedi, R. P., Lewandrowski, U., Wiesner, J., Wortelkamp, S., Moebius, J., Schütz, C., Walter, U., Gambaryan, S., and Sickmann, A. (2008) Phosphoproteome of resting human platelets. *J. Proteome Res.* **7,** 526–534
23. Ferrary, E., Cohen-Tannoudji, M., Pehau-Arnaudet, G., Lapillonne, A., Athman, R., Ruiz, T., Boulouha, L., El Marjou, F., Doye, A., Fontaine, J. J., Antony, C., Babinet, C., Louvard, D., Jaisser, F., and Robine, S. (1999) In vivo, villin is required for Ca^{2+}-dependent F-actin disruption in intestinal brush borders. *J. Cell Biol.* **146,** 819–830
24. Naik, U. P., and Naik, M. U. (2003) Association of CIB with GPIIb/IIIa during outside-in signaling is required for platelet spreading on fibrinogen. *Blood* **102,** 1355–1362
25. Chen, J., and López, J. A. (2005) Interactions of platelets with subendothelium and endothelium. *Microcirculation* **12,** 235–246
26. Remijn, J. A., Wu, Y. P., Jeninga, E. H., IJsseldijk, M. J., van Willigen, G., de Groot, P. G., Sixma, J. J., Nurden, A. T., and Nurden, P. (2002) Role of ADP receptor P2Y(12) in platelet adhesion and thrombus formation in flowing blood. *Arterioscler. Thromb. Vasc. Biol.* **22,** 686–691

27. Shattil, S. J., and Newman, P. J. (2004) Integrins. Dynamic scaffolds for adhesion and signaling in platelets. *Blood* **104,** 1606–1615
28. Flevaris, P., Stojanovic, A., Gong, H., Chishti, A., Welch, E., and Du, X. (2007) A molecular switch that controls cell spreading and retraction. *J. Cell Biol.* **179,** 553–565
29. Chen, Y. P., O'Toole, T. E., Shipley, T., Forsyth, J., LaFlamme, S. E., Yamada, K. M., Shattil, S. J., and Ginsberg, M. H. (1994) "Inside-out" signal transduction inhibited by isolated integrin cytoplasmic domains. *J. Biol. Chem.* **269,** 18307–18310
30. Law, D. A., Nannizzi-Alaimo, L., and Phillips, D. R. (1996) Outside-in integrin signal transduction. αIIb β3-(GP IIb IIIa) tyrosine phosphorylation induced by platelet aggregation. *J. Biol. Chem.* **271,** 10811–10815
31. Shattil, S. J., Kashiwagi, H., and Pampori, N. (1998) Integrin signaling. The platelet paradigm. *Blood* **91,** 2645–2657
32. Zhang, G., Xiang, B., Ye, S., Chrzanowska-Wodnicka, M., Morris, A. J., Gartner, T. K., Whiteheart, S. W., White, G. C., 2nd, Smyth, S. S., and Li, Z. (2011) Distinct roles for Rap1b protein in platelet secretion and integrin αIIbβ3 outside-in signaling. *J. Biol. Chem.* **286,** 39466–39477
33. Jantzen, H. M., Milstone, D. S., Gousset, L., Conley, P. B., and Mortensen, R. M. (2001) Impaired activation of murine platelets lacking Gα_{i2}. *J. Clin. Invest.* **108,** 477–483
34. El-Daher, S. S., Patel, Y., Siddiqua, A., Hassock, S., Edmunds, S., Maddison, B., Patel, G., Goulding, D., Lupu, F., Wojcikiewicz, R. J., and Authi, K. S. (2000) Distinct localization and function of (1,4,5)IP(3) receptor subtypes and the (1,3,4,5)IP(4) receptor GAP1(IP4BP) in highly purified human platelet membranes. *Blood* **95,** 3412–3422
35. van Nispen Tot Pannerden, H. E., van Dijk, S. M., Du, V., and Heijnen, H. F. (2009) Platelet protein-disulfide isomerase is localized in the dense tubular system and does not become surface expressed after activation. *Blood* **114,** 4738–4740
36. Yu, J. C., Lloyd-Burton, S. M., Irvine, R. F., and Schell, M. J. (2005) Regulation of the localization and activity of inositol 1,4,5-trisphosphate 3-kinase B in intact cells by proteolysis. *Biochem. J.* **392,** 435–441
37. Soriano, S., and Banting, G. (1997) Possible roles of inositol 1,4,5-trisphosphate 3-kinase B in calcium homeostasis. *FEBS Lett.* **403,** 1–4
38. Xia, H. J., and Yang, G. (2005) Inositol 1,4,5-trisphosphate 3-kinases. Functions and regulations. *Cell Res.* **15,** 83–91
39. Zhu, D. M., Tekle, E., Huang, C. Y., and Chock, P. B. (2000) Inositol tetrakisphosphate as a frequency regulator in calcium oscillations in HeLa cells. *J. Biol. Chem.* **275,** 6063–6066
40. da Silva, C. P., Emmrich, F., and Guse, A. H. (1994) Adriamycin inhibits inositol 1,4,5-trisphosphate 3-kinase activity *in vitro* and blocks formation of inositol 1,3,4,5-tetrakisphosphate in stimulated Jurkat T-lymphocytes. Does inositol 1,3,4,5-tetrakisphosphate play a role in Ca^{2+}-entry? *J. Biol. Chem.* **269,** 12521–12526
41. Kim, S. H., Lim, K. M., Noh, J. Y., Kim, K., Kang, S., Chang, Y. K., Shin, S., and Chung, J. H. (2011) Doxorubicin-induced platelet procoagulant activities. An important clue for chemotherapy-associated thrombosis. *Toxicol. Sci.* **124,** 215–224
42. Bennett, V., and Gilligan, D. M. (1993) The spectrin-based membrane skeleton and micron-scale organization of the plasma membrane. *Annu. Rev. Cell Biol.* **9,** 27–66
43. Gilligan, D. M., Sarid, R., and Weese, J. (2002) Adducin in platelets. Activation-induced phosphorylation by PKC and proteolysis by calpain. *Blood* **99,** 2418–2426
44. Käser-Glanzmann, R., Jakábová, M., George, J. N., and Lüscher, E. F. (1978) Further characterization of calcium-accumulating vesicles from human blood platelets. *Biochim. Biophys. Acta* **512,** 1–12
45. Cutler, L., Rodan, G., and Feinstein, M. B. (1978) Cytochemical localization of adenylate cyclase and of calcium ion, magnesium ion-activated ATPases in the dense tubular system of human blood platelets. *Biochim. Biophys. Acta* **542,** 357–371
46. Menashi, S., Davis, C., and Crawford, N. (1982) Calcium uptake associated with an intracellular membrane fraction prepared from human blood platelets by high-voltage, free-flow electrophoresis. *FEBS Lett.* **140,** 298–302
47. Dean, W. L. (1984) Purification and reconstitution of a Ca^{2+} pump from human platelets. *J. Biol. Chem.* **259,** 7343–7348
48. Enouf, J., Bredoux, R., Bourdeau, N., Sarkadi, B., and Levy-Toledano, S. (1989) Further characterization of the plasma membrane- and intracellular membrane-associated platelet Ca^{2+} transport systems. *Biochem. J.* **263,** 547–552
49. Rybicki, J. P., Venton, D. L., and Le Breton, G. C. (1983) The thromboxane antagonist, 13-azaprostanoic acid, inhibits arachidonic acid-induced Ca^{2+} release from isolated platelet membrane vesicles. *Biochim. Biophys. Acta* **751,** 66–73
50. Varga-Szabo, D., Braun, A., and Nieswandt, B. (2009) Calcium signaling in platelets. *J. Thromb. Haemost.* **7,** 1057–1066
51. Reed, G. L., Fitzgerald, M. L., and Polgár, J. (2000) Molecular mechanisms of platelet exocytosis. Insights into the "secrete" life of thrombocytes. *Blood* **96,** 3334–3342
52. Blair, P., and Flaumenhaft, R. (2009) Platelet α-granules. Basic biology and clinical correlates. *Blood Rev.* **23,** 177–189
53. Nalaskowski, M. M., Fliegert, R., Ernst, O., Brehm, M. A., Fanick, W., Windhorst, S., Lin, H., Giehler, S., Hein, J., Lin, Y. N., and Mayr, G. W. (2011) Human inositol 1,4,5-trisphosphate 3-kinase isoform B (IP3KB) is a nucleocytoplasmic shuttling protein specifically enriched at cortical actin filaments and at invaginations of the nuclear envelope. *J. Biol. Chem.* **286,** 4500–4510
54. Lloyd-Burton, S. M., Yu, J. C., Irvine, R. F., and Schell, M. J. (2007) Regulation of inositol 1,4,5-trisphosphate 3-kinases by calcium and localization in cells. *J. Biol. Chem.* **282,** 9526–9535
55. Gregg, D., and Goldschmidt-Clermont, P. J. (2003) Cardiology patient page. Platelets and cardiovascular disease. *Circulation* **108,** e88–90
56. El Haouari, M., and Rosado, J. A. (2008) Platelet signalling abnormalities in patients with type 2 diabetes mellitus. A review. *Blood Cells. Mol. Dis.* **41,** 119–123
57. El Haouari, M., and Rosado, J. A. (2009) Platelet function in hypertension. *Blood Cells Mol. Dis.* **42,** 38–43